Research
3D Printing—Review

Engineering 2015, 1(2): 261–268
DOI 10.15302/J-ENG-2015061

Design and 3D Printing of Scaffolds and Tissues

Jia An, Joanne Ee Mei Teoh, Ratima Suntornnond, Chee Kai Chua*

ABSTRACT A growing number of three-dimensional (3D)-printing processes have been applied to tissue engineering. This paper presents a state-of-the-art study of 3D-printing technologies for tissue-engineering applications, with particular focus on the development of a computer-aided scaffold design system; the direct 3D printing of functionally graded scaffolds; the modeling of selective laser sintering (SLS) and fused deposition modeling (FDM) processes; the indirect additive manufacturing of scaffolds, with both micro and macro features; the development of a bioreactor; and 3D/4D bioprinting. Technological limitations will be discussed so as to highlight the possibility of future improvements for new 3D-printing methodologies for tissue engineering.

KEYWORDS rapid prototyping, 3D printing, additive manufacturing, tissue engineering, bioprinting

1 Introduction

The concept of tissue engineering was formalized in 1993 when Langer and Vacanti published a historical milestone paper in *Science*, in which the characteristics and applications of biodegradable three-dimensional (3D) scaffolds were first detailed [1]. Ideally, 3D scaffolds should be highly porous, have well-interconnected pore networks, and have consistent and adequate pore size for cell migration and infiltration [2]. In the decade following the publication of this paper (1993–2002), a number of conventional manufacturing techniques were applied to fabricating porous 3D scaffolds, such as fiber bonding, phase separation, solvent casting, particulate leaching, membrane lamination, molding, and foaming [3]. However, all these methods share a major drawback: They do not permit enough control of scaffold architecture, pore network, and pore size, giving rise to inconsistent and less-than-ideal 3D scaffolds. To overcome this problem, researchers proposed the use of 3D-printing methods (also known as rapid prototyping, solid free-form fabrication, or additive manufacturing) to fabricate customized scaffolds with controlled pore size and pore structure [4–6]. Out of more than 40 different 3D-printing techniques in development, fused deposition modeling (FDM), stereolithography, inkjet printing, selective laser sintering (SLS), and colorjet printing appeared to be the most popular, due to their ability to process plastics [7, 8]. As a result, in the second decade of this field (2003–2012), the number of studies in the arena of 3D printing for tissue engineering rapidly multiplied. These studies covered scaffold design, process modeling and optimization, comparisons of 3D-printing methods, post-processing and characterization of 3D printed scaffolds, *in vitro* and *in vivo* applications of 3D printed scaffolds, new scaffold materials for 3D printing, new 3D-printing methods for scaffold fabrication, and even the branching out of an entirely new field—3D bioprinting, or organ printing. Our research group has been extensively involved in this vast wave of research. In this paper, we present our past and current work in this field, and give our perspective on the future of this area as it moves into its third decade (2013–2022).

2 Scaffold architecture design

2.1 Scaffold library

Scaffold architecture design can significantly influence both mechanical property and cell behaviors [9]. We have adopted a bottom-up approach when constructing a 3D scaffold; that is, first making unit cells, and then assembling them into a 3D scaffold. Using this approach, we can fine-tune the mechanical property, based on the porous structure design. We have developed in-house a computer-aided system for tissue scaffolds (CASTS) that can automatically create a highly porous 3D scaffold model with controlled architecture, and precisely match the external surface profile of a native anatomic structure such as bone [10–12]. In this system, nearly 20 polyhedral shapes are selected to form the basic geometry of a unit cell. The scaffold library and the parameters of each unit cell, such as pore size and strut size, can be adjusted, and each polyhedral unit can be repeated automatically in a spatial arrangement and sized to form a block that suits the intended scaffold application (Figure 1). An anatomically shaped porous scaffold can then be created through Bool-

Singapore Centre for 3D Printing, School of Mechanical and Aerospace Engineering, Nanyang Technological University, Singapore 639798, Singapore
* Correspondence author. E-mail: mckchua@ntu.edu.sg
Received 30 January 2015; received in revised form 23 March 2015; accepted 30 June 2015

ean operation between the scaffold block and the actual surface model of the defect tissue. A detailed derivation of the mathematical formulae of the CASTS system for designing and fabricating tissue engineering scaffolds is contained in Ref. [13].

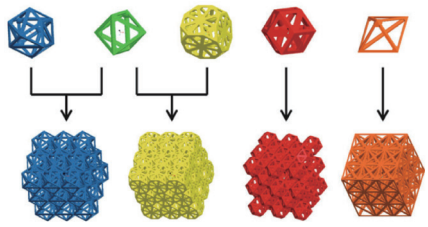

Figure 1. An example of five polyhedral units and their resultant blocks, generated in the CASTS scaffold library.

2.2 Functionally graded scaffold

Natural tissues such as bone usually have a gradient porous structure, so matching mechanical strength and stiffness between porous scaffold design and the target tissue structure is important [14]. There are two types of stiffness gradient in bones: radial gradients in long bones, and linear gradients in short and irregular bones. We have achieved radial gradient design by arranging cylindrical unit cells in a concentric manner so that the porosity decreases linearly from the center to the periphery. This linear gradient occurs as a result of varying the strut diameter along the gradient direction. Therefore, we can tailor the stiffness variation for CASTS scaffolds by adjusting the porosity-stiffness relationship [15]. After modifying and improving the CASTS system, our group successfully fabricated a human mandibular cancellous bone scaffold and a femur bone segment, both with functional gradients [16, 17]. An example of a functionally graded femur bone segment is shown in Figure 2. This process is highly accurate and reproducible. Another method of designing gradient structure is based on shape function and on an all-hexahedral mesh refinement [18]. In this method, a truncated bone is subdivided and represented using various irregular hexahedral elements, which are then converted into various irregular pore elements based on shape function. The entire pore model is obtained after a union operation among the irregular pores, and then the resulting bone scaffold is obtained by performing a difference operation between the contour model and the pore model. Using this method, a well-defined pore size distribution can be achieved for gradient bone-scaffold design. Recently, a new method based on sigmoid function and Gaussian radial basis function has been developed to generate functionally graded structures, and the resulting models can be exported as STL-files and be 3D printed [19].

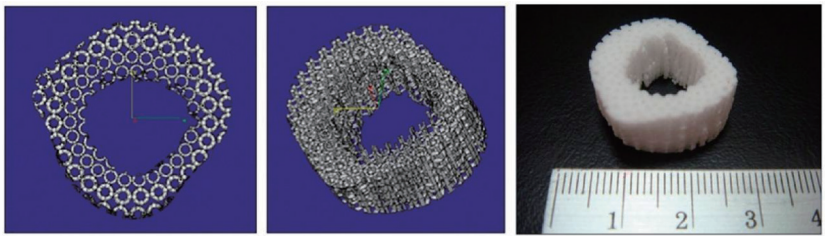

Figure 2. Virtual and physical prototypes of the functionally graded porous scaffold of a femur bone segment.

2.3 Design for vascularization

In addition to mechanical performance, vascularization is a major limitation in tissue engineering, especially when engineering thick or bulk tissues. Researchers have proposed various strategies to enhance or accelerate vascularization, in which scaffold design plays a crucial role [20]. Results show that a designed pore size of 250 μm or above favors the growth of blood vessels more than smaller pore sizes [21]. Also, a high porosity does not necessarily lead to more vascularization, because cell migration and vascularization could be inhibited if there is little interconnectivity between pores [22]. Recently, researchers have developed a tool box for evaluating 3D porous scaffolds [23]. This tool box is based on modular scaffold design, and allows the fine-tuning of scaffold pore size and porosity for vascularization study. Our group is exploring a new concept of hybrid scaffold design to address the vascularization issue. This new approach involves thin porous membranes and filament meshes that alternate in layers to form a 3D scaffold (Figure 3) [24].

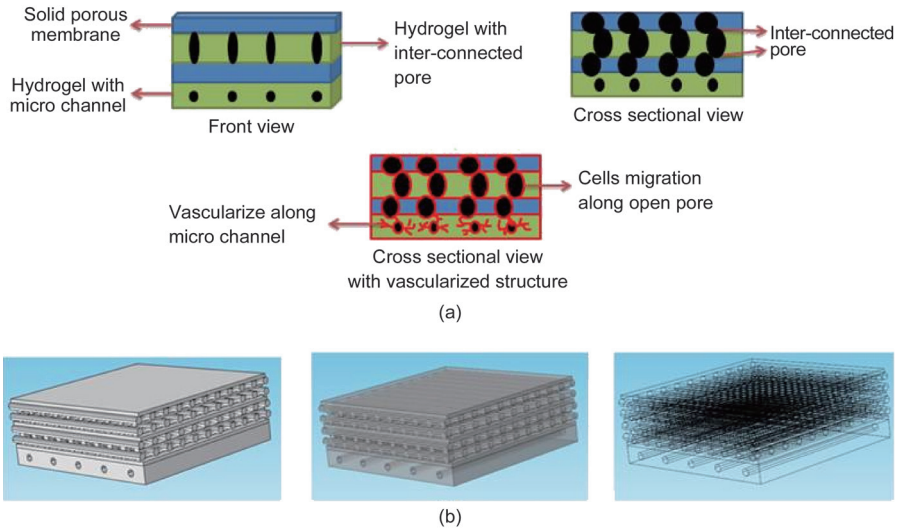

Figure 3. A proposed hybrid scaffold design for vascularization.

3 Direct 3D printing

3.1 Specific forms of materials

At room temperature, the primary forms of materials used for 3D printing are solidifiable fluid, non-brittle filament, laminated thin sheet, and fine powder (see Table 1) [25]. Each form is specific for certain 3D-printing processes. If a material

is deemed suitable for a particular application but cannot be easily prepared in the specific form required by the desired 3D-printing process, printing this material would be a challenge. Even if a material can be prepared in a specific form, this does not guarantee that the material is 3D printable, because successful printing in the vertical dimension also relies on the bonding strength between layers. Therefore, when exploring a material for 3D scaffold applications, it is important to consider the available forms of the material at the very first stage. Furthermore, in order to increase the range of 3D printable biomaterials, future development should include the invention of new methods to transform existing biomaterials into suitable forms for 3D printing. For example, gelatin gel is solidifiable upon a decrease in temperature, but this low-temperature environment conflicts with what is favorable for cell survival. Therefore, future research may involve the development of a new mechanism of solidification for gelatin, such as solidification by enzymatic crosslinking [26], or the development of a new hybrid mechanism for low-temperature deposition of hydrogels and cells [27].

Table 1. Specific forms of materials and suitable 3D-printing processes.

Form	Examples	Suitable 3D-printing processes	Refs.
Solidifiable fluid	Photopolymer resins, temperature sensitive polymers, ion cross-linkable hydrogels, ceramic paste, etc.	Stereolithography (SLA)	[28]
		Polyjet	[29, 30]
		Digital light processing (DLP)	[31]
		Micro-extrusion	[32]
Non-brittle filament	Thermoplastics, e.g., ABS, PLA, and PCL	Fused deposition modeling (FDM)	[33]
Laminated thin sheet	Paper, plastic sheet, metal foil	Paper lamination technology (PLT)	[34]
		Laminated object manufacturing (LOM)	[35]
		Ultrasonic consolidation (UC)	[36]
Fine powder	Plastic fine powder, ceramic powder, metal powder	Selective laser sintering/melting (SLS/SLM)	[17, 37, 38]
		Electron beam melting (EBM)	[39]
		Laser engineered net shaping (LENS)	[40]
		Direct metal deposition (DMD)	[41]
		Colorjet printing (CJP)	[42–44]

Notes: ABS—acrylonitrile-butadiene-styrene; PLA—polylactic acid; PCL—polycaprolactone.

3.2 Process parameters and limitations

Our group investigated a range of materials using the SLS process for fabricating tissue-engineering scaffolds. Table 2 summarizes the main process parameters for SLS, namely part-bed temperature, laser power, and scan speed. In particular, in the polyetheretherketone/hydroxyapatite (PEEK/HA) system, results show that HA should be kept at 40 wt.% or below in order to ensure structural integrity. In the polyvinyl alcohol/hydroxyapatite (PVA/HA) and polycaprolactone/hydroxyapatite (PCL/HA) systems, HA should be kept at 30 wt.% or below in order to yield successful scaffold specimens with well-defined pore interconnectivity and good structural integrity. When developing composite material systems, although the addition of HA initially improved mechanical properties and bioactivity, it compromised material properties during the hydrolytic degradation process [45]. In addition to scaffolds, we investigated laser sintering of drug delivery devices and their microfeatures [46–48].

Table 2. SLS process parameters for different types of polymers.

Polymer type	Composition (wt.%)	Part-bed temperature (°C)	Laser powder (W)	Scan speed ($mm \cdot s^{-1}$)	Refs.
PCL	100	30–55	1–7	3810–5080	[49]
PLLA	100	60	10–15	1270	[49]
PVA	100	60–65	10–15	1270–5080	[49]
PLGA	100	70	10	1651	[50]
PEEK	100	110–140	9–28	5080	[49]
PEEK/HA	> 60/40	140	16	5080	[51, 52]
PVA/HA	> 70/30	65–80	13–15	1270–1778	[53, 54]
PCL/HA	> 70/30	40	3	1270–2540	[55]

Notes: PLLA—poly-*L*-lactic acid; PLGA—poly(lactic-*co*-glycolic acid).

One limitation in the SLS process is material wastage when building small prototypes such as tissue-engineering scaffolds. However, this problem can be overcome by incorporating a compact adaptation system into the SLS part bed, allowing the adaptor to transfer the motion of the SLS part bed onto its own small part bed [56]. Up to 6.5 times the amount of powder can be saved by using this device. A second limitation of SLS-made scaffolds is the low retention of cells during cell seeding. One reason is that the materials used for SLS are synthetic and do not favor initial cell at-

tachment. The other reason is that the pores are much larger than cells due to SLS resolution issue, as a result, cells fall through the pores during the seeding process. However, the use of a hybrid 3D scaffold that consists of alternate electrospun nanofibers and 3D printed scaffold layers will prevent cells from falling through, due to the small size of the nanofiber pores [57, 58]. An alternative solution is to inject cell-laden collagen hydrogel into the porous structure [59]. An unresolved limitation in SLS scaffolds does exist, for example, the entrapment of powder in the interior region of the porous scaffold. It is difficult to remove the entrapped powder manually, especially for pore sizes below 500 μm. Researchers have explored ultrasonic cleaning with only limited success [60].

3.3 Modeling for FDM and SLS

In 3D printing, it is important to understand the process itself, as well as the science behind it, in order to improve the process further (Figure 4). PCL is a representative biomaterial for the FDM process. The results from modeling and finite element analysis indicate that the pressure drop and the velocity of the PCL melt flow depend on the flow channel parameters [61]. The temperature gradient of the PCL melt shows that it liquefies within 35% of the channel length [61]. Similarly, we modeled the heat-transfer phenomena during the SLS process. By incorporating material properties such as thermal conductivity, thermal diffusivity, surface reflectivity, and absorption coefficient, our model helped to identify the biomaterial and laser-beam properties that are critical to the sintering result [62]. It is also important to understand the relationship between mechanical properties and scaffold porosity in 3D printing (Figure 5). We obtained such a plot for FDM, based on experimental data from ABS samples [63, 64]. In addition, we found a feasible porosity and compressive stiffness range for our CASTS-designed PCL scaffolds via the testing of physical prototypes [65]. This stiffness range fairly matches the stiffness gradient of cancellous bone in the maxillofacial region, which varies gradually from 35.55 MPa in the molar region to 67.48 MPa in the incisor and canine region [66].

4 Indirect 3D printing

Natural polymers usually have very good biocompatibility, and can provide a favorable micro-environment for cells as compared to synthetic polymers. However, the 3D printability of natural polymers is generally poor. Indirect 3D printing was developed in order to produce a 3D porous scaffold

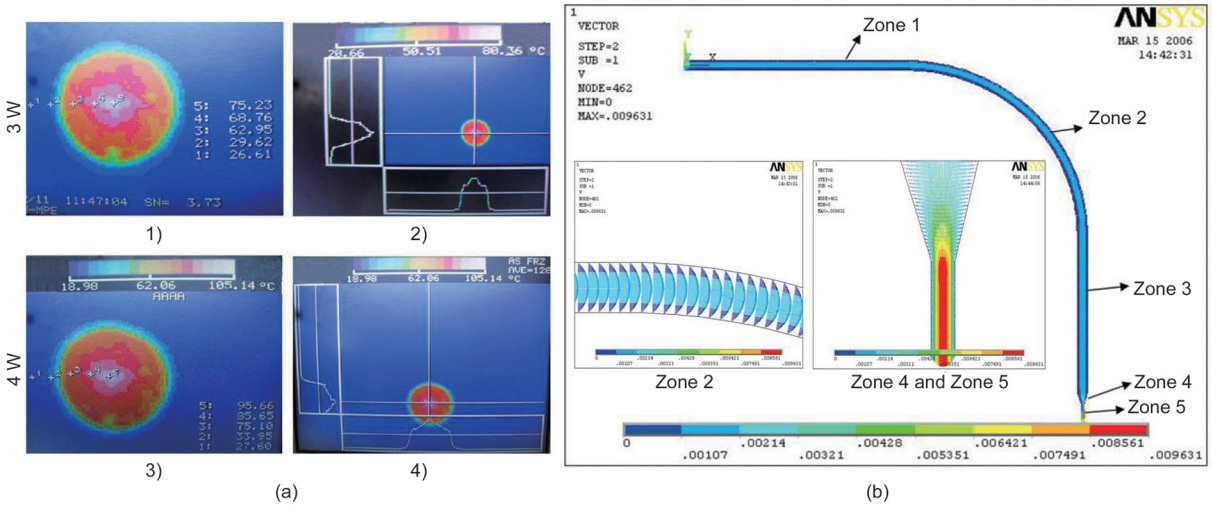

Figure 4. Process modelling. (a) Temperature distribution and Gaussian contour in the laser sintering process: 1), 3) are temperature distributions; 2), 4) are Gaussian contours. (b) Velocity profiles at different zones along the melt flow channel.

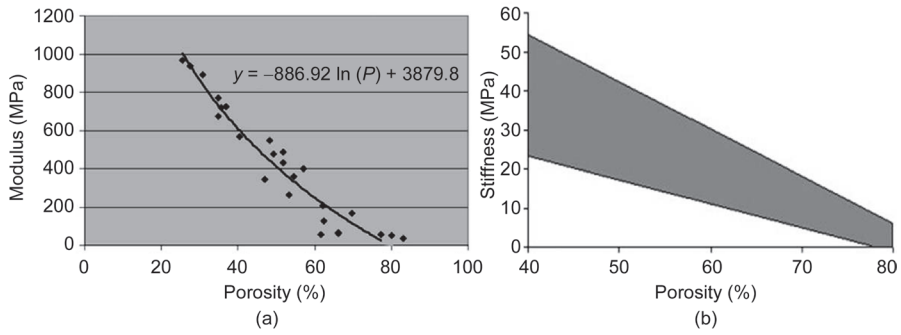

Figure 5. Scaffold porosity and mechanical property. (a) Relationship between porosity and modulus in FDM scaffolds; (b) the feasible porosity and compressive stiffness range (gray band) in SLS-made PCL scaffolds.

using natural polymers such as collagen or gelatin. In contrast to direct 3D printing, which produces a scaffold directly from the model material, indirect 3D printing creates a negative mold, usually from a support material, and then casts the desired polymer scaffold out of the mold via a drying method [6, 67, 68]. Collagen scaffolds with 3D networks of internal channels can be produced using this approach [69]. Moreover, freeze-drying was found to be the most suitable drying method in indirect

3D printing, as it induced less shrinkage than critical-point drying, and accurately reproduced the design morphology of the channels [69]. Furthermore, indirect fabrication can be combined with a foaming process to produce highly and uniformly porous gelatin scaffolds with complex channel architectures [29, 70], as shown in Figure 6(a–d). The order of this structure can be improved further by incorporating monodispersed microspheres into the casting process [71], as shown in Figure 6(e, f). In addition to collagen and gelatin, our group has successfully produced porous scaffolds from silk fibroin protein with both macro- and micro-morphological features [30, 72].

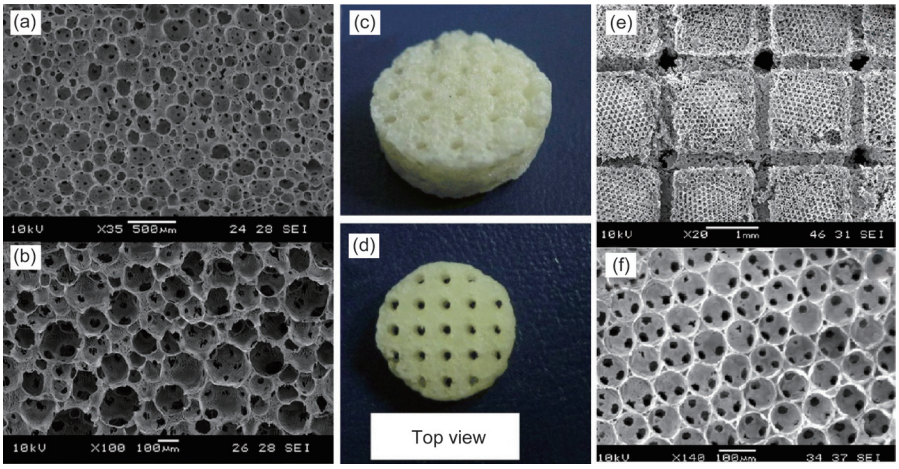

Figure 6. Highly and uniformly porous interconnected network via the combination of indirect 3D printing and foaming processes

5 Bioreactor

A bioreactor is an important post-processing tool in tissue engineering, as it provides a dynamic environment for cell-scaffold construct, and facilitates the maturation of the construct. More importantly, a bioreactor is a part of the automation line in industry-scale tissue engineering [73]. A recent study reports that scaffold architecture could influence cell differentiation in a bioreactor, but not in static culture [74], further evidencing the importance of a bioreactor's role. Surprisingly, by taking the advantage of the air-liquid interface commonly found in a rotating bioreactor, induced pluripotent stem (iPS) cells can be induced toward the differentiation of alveolar epithelium, offering a new role for a bioreactor in resolving a cell-source problem [75]. The most recent bioreactor design is a dual-flow bioreactor coupled with mechanical stimulation [76]. This novel design allows nutrients, anabolic or catabolic factors to diffuse from one side of the construct, enabling the creation of gradients; as a result, this bioreactor design is well suited for engineering interface tissues. Our group has focused particularly on the effect of interstitial flow on fibroblast responses [77]. Through a computational fluid dynamics study, we found that dynamic flow, even a flow rate as low as 0.002 $cm \cdot s^{-1}$, can support much better mass exchange, higher cell number, and more even cell and nutrient distribution than static culture [78]. We have also developed a dual-window dual-bandwidth spectroscopic optical-coherence tomography (DWDB-SOCT) technique to monitor fibroblast cell proliferation in scaffolds. Fibroblasts and their distribution in scaffolds are clearly differentiable in the spectroscopic images [79]. In future, we expect that bioreactors will play more biological roles and take on a more integrated design by combining various types of stimulation and non-invasive monitoring techniques.

6 3D bioprinting and beyond

One of the major advances in tissue engineering is the emergence of a new field: 3D bioprinting [80]. Mironov et al. [81] originally proposed the concept of 3D bioprinting as "organ printing," and defined it as the computer-aided, jet-based 3D tissue-engineering of living human organs. This organ printing process exactly follows the typical process chain of 3D printing; that is, starting with a computer-aided design (CAD) model, converting to a STL file, slicing and then printing. The major advantages of organ printing are automation and high cell density, compared to a traditional scaffold-based approach [82]. The materials used for organ printing are microtissues, usually in the form of spheroids. These closely placed spheroids can undergo self-assembly and fuse together [83], forming the foundation of 3D printability in organ printing. Organ printing carries the imminent potential to address organization and complexity issues in engineered tissues [84]. It also carries great potential to foster the establishment of an industry-scale robotic tissue-fabrication line [73]. Nevertheless, current application of organ printing is limited to *in vitro* drug testing. According to Mironov, the first bioprinted organ transplant in the world is likely to be the thyroid gland of a mouse, in 2015 [85].

Besides organ printing, other elegant bioprinting approaches and methodologies exist, such as inkjet printing, micro-extrusion and laser-assisted forward transfer, which are comprehensively reviewed in Ref. [86]. It is a major challenge in these approaches to position and culture multiple types of cells in a single process at a defined location. Although researchers have obtained initial success in printing heterogeneous tissues [87, 88], these were printed in separate compartments and did not replicate the microstructure of the native tissue. To address this challenge, our group plans to focus on a fundamental study of the bioprinting process, such as developing a time-pressure model to precisely control extruded material [89].

One interesting derivation of 3D bioprinting is the integration of microelectronic and mechatronic components. For example, a bio-bot is a walking robot powered by the contraction of a strip of mammalian skeletal muscle cells [90]. Another interesting derivation of 3D bioprinting is the concept of 4D bio-

printing. 4D printing refers to the 3D printing of programmable materials; since the printed part gradually transforms in shape over the post-printing period, the fourth dimension refers to time [91]. One physical demonstration of 4D printing involved intelligent active hinges that enabled origami folding [92], and this concept has been extended further to make light-responsive windows that open and close automatically in response to the amount of sunshine. Therefore, the research community considers 4D printing to be a new and emerging field [93]. Our group is currently collaborating with Stratasys (www.stratasys.com) to work on 4D-printable shape-memory polymers [94]. In terms of 4D bioprinting, the development of programmable biomaterials appears to be crucial in realizing time-dependent shape change. The term "4D bioprinting" is currently less defined than that of 4D printing, and the shape it will take in the future is largely unknown, but well worth watching.

7 Future prospects

In the second decade after the birth of tissue engineering, 3D printing gradually became a definite part of this field, due to its controllability and manufacturing capability. Looking into the future, even once the technical challenges described above are overcome, it will still be a long way from transforming academic know-how into clinical products that benefit society. Researchers' current tasks in the field are to accelerate the standardization and certification of 3D printed medical devices. A prolonged delay in this standardization would make regulatory work even more complicated, especially with the currently trending and transforming 3D bioprinting technologies, because the definition of "medical device" may soon be redefined. Another future trend may come in the legal landscape [95], as the infringement and protection of intellectual properties around 3D printing interweave more intensely. Thus, an early and informed exploration of various legal approaches could be the best preparation to cope with tomorrow's changes.

Acknowledgements

The authors would like to thank Singapore National Research Foundation (NRF) for funding the Singapore Centre for 3D Printing (SC3DP). The authors would also like to thank Professor Li Lin at the University of Manchester for his kind invitation for submission.

Compliance with ethics guidelines

Jia An, Joanne Ee Mei Teoh, Ratima Suntornnond, and Chee Kai Chua declare that they have no conflict of interest or financial conflicts to disclose.

References

1. R. Langer, J. P. Vacanti. Tissue engineering. *Science*, 1993, 260(5110): 920–926
2. Q. L. Loh, C. Choong. Three-dimensional scaffolds for tissue engineering applications: Role of porosity and pore size. *Tissue Eng. Part B Rev.*, 2013, 19(6): 485–502
3. S. Yang, K. F. Leong, Z. Du, C. K. Chua. The design of scaffolds for use in tissue engineering. Part I. Traditional factors. *Tissue Eng.*, 2001, 7(6): 679–689
4. S. Yang, K. F. Leong, Z. Du, C. K. Chua. The design of scaffolds for use in tissue engineering. Part II. Rapid prototyping techniques. *Tissue Eng.*, 2002, 8(1): 1–11
5. K. F. Leong, C. M. Cheah, C. K. Chua. Solid freeform fabrication of three-dimensional scaffolds for engineering replacement tissues and organs. *Biomaterials*, 2003, 24(13): 2363–2378
6. W. Y. Yeong, C. K. Chua, K. F. Leong, M. Chandrasekaran. Rapid prototyping in tissue engineering: Challenges and potential. *Trends Biotechnol.*, 2004, 22(12): 643–652
7. T. Boland, et al. Rapid, prototyping of artificial tissues and medical devices. *Adv. Mater. Process.*, 2007, 165(4): 51–53
8. P. J. Bártolo, C. K. Chua, H. A. Almeida, S. M. Chou, A. S. C. Lim. Biomanufacturing for tissue engineering: Present and future trends. *Virtual and Physical Prototyping*, 2009, 4(4): 203–216
9. S. J. Hollister. Porous scaffold design for tissue engineering. *Nat. Mater.*, 2005, 4(7): 518–524
10. C. M. Cheah, C. K. Chua, K. F. Leong, S. W. Chua. Development of a tissue engineering scaffold structure library for rapid prototyping. Part 1: Investigation and classification. *Int. J. Adv. Manuf. Technol.*, 2003, 21(4): 291–301
11. C. M. Cheah, C. K. Chua, K. F. Leong, S. W. Chua. Development of a tissue engineering scaffold structure library for rapid prototyping. Part 2: Parametric library and assembly program. *Int. J. Adv. Manuf. Technol.*, 2003, 21(4): 302–312
12. C. M. Cheah, C. K. Chua, K. F. Leong, C. H. Cheong, M. W. Naing. Automatic algorithm for generating complex polyhedral scaffold structures for tissue engineering. *Tissue Eng.*, 2004, 10(3–4): 595–610
13. M. W. Naing, C. K. Chua, K. F. Leong, Y. Wang. Fabrication of customised scaffolds using computer-aided design and rapid prototyping techniques. *Rapid Prototyping J.*, 2005, 11(4): 249–259
14. K. F. Leong, C. K. Chua, N. Sudarmadji, W. Y. Yeong. Engineering functionally graded tissue engineering scaffolds. *J. Mech. Behav. Biomed. Mater.*, 2008, 1(2): 140–152
15. N. Sudarmadji, C. K. Chua, K. F. Leong. The development of computer-aided system for tissue scaffolds (CASTS) system for functionally graded tissue-engineering scaffolds. *Methods Mol. Biol.*, 2012, 868: 111–123
16. C. K. Chua, N. Sudarmadji, K. F. Leong, S. M. Chou, S. C. Lim, W. M. Firdaus. Process flow for designing functionally graded tissue engineering scaffolds. In: *Innovative Developments in Design and Manufacturing—Advanced Research in Virtual and Rapid Prototyping*, 2010: 45–49
17. C. K. Chua, K. F. Leong, N. Sudarmadji, M. J. J. Liu, S. M. Chou. Selective laser sintering of functionally graded tissue scaffolds. *MRS Bull.*, 2011, 36(12): 1006–1014
18. S. Cai, J. Xi, C. K. Chua. A novel bone scaffold design approach based on shape function and all-hexahedral mesh refinement. *Methods in Molecular Biology*, 2012, 868: 45–55
19. N. Yang, Z. Quan, D. Zhang, Y. Tian. Multi-morphology transition hybridization CAD design of minimal surface porous structures for use in tissue engineering. *Comput. Aided Design*, 2014, 56: 11–21
20. J. Rouwkema, N. C. Rivron, C. A. van Blitterswijk. Vascularization in tissue engineering. *Trends Biotechnol.*, 2008, 26(8): 434–441
21. D. Druecke, et al. Neovascularization of poly(ether ester) block-copolymer scaffolds *in vivo*: Long-term investigations using intravital fluorescent microscopy. *J. Biomed. Mater. Res. A*, 2004, 68A(1): 10–18
22. V. Karageorgiou, D. Kaplan. Porosity of 3D biomaterial scaffolds and osteogenesis. *Biomaterials*, 2005, 26(27): 5474–5491

23. M. O. Wang, et al. Evaluating 3D-printed biomaterials as scaffolds for vascularized bone tissue engineering. *Adv. Mater.*, 2015, 27(1): 138–144
24. R. Suntornnond, J. An, W. Y. Yeong, C. K. Chua. Hybrid membrane based structure: A novel approach for tissue engineering scaffold. In: *The 4th International Conference on Additive Manufacturing and Bio-manufacturing (ICAM-BM 2014)*. Beijing, China, 2014: 41–42
25. C. K. Chua, K. F. Leong. *3D Printing and Additive Manufacturing: Principles and Applications*. Singapore: World Scientific Publishing Company Pte Limited, 2014
26. C. W. Yung, L. Q. Wu, J. A. Tullman, G. F. Payne, W. E. Bentley, T. A. Barbari. Transglutaminase crosslinked gelatin as a tissue engineering scaffold. *J. Biomed. Mater. Res. A*, 2007, 83A(4): 1039–1046
27. Y. Yan, et al. Direct construction of a three-dimensional structure with cells and hydrogel. *J. Bioact. Compat. Pol.*, 2005, 20(3): 259–269
28. F. P. Melchels, J. Feijen, D. W. Grijpma. A poly(*D*,*L*-lactide) resin for the preparation of tissue engineering scaffolds by stereolithography. *Biomaterials*, 2009, 30(23–24): 3801–3809
29. J. Y. Tan, C. K. Chua, K. F. Leong. Indirect fabrication of gelatin scaffolds using rapid prototyping technology. *Virtual and Physical Prototyping*, 2010, 5(1): 45–53
30. M. J. J. Liu, S. M. Chou, C. K. Chua, B. C. M. Tay, B. K. Ng. The development of silk fibroin scaffolds using an indirect rapid prototyping approach: Morphological analysis and cell growth monitoring by spectral-domain optical coherence tomography. *Med. Eng. Phys.*, 2013, 35(2): 253–262
31. D. Dean, et al. Multiple initiators and dyes for continuous Digital Light Processing (cDLP) additive manufacture of resorbable bone tissue engineering scaffolds: A new method and new material to fabricate resorbable scaffold for bone tissue engineering via continuous Digital Light Processing. *Virtual and Physical Prototyping*, 2014, 9(1): 3–9
32. C. Wu, et al. 3D-printing of highly uniform $CaSiO_3$ ceramic scaffolds: Preparation, characterization and *in vivo* osteogenesis. *J. Mater. Chem.*, 2012, 22(24): 12288–12295
33. D. W. Hutmacher, T. Schantz, I. Zein, K. W. Ng, S. H. Teoh, K. C. Tan. Mechanical properties and cell cultural response of polycaprolactone scaffolds designed and fabricated via fused deposition modeling. *J. Biomed. Mater. Res.*, 2001, 55(2): 203–216
34. G. Yu, Y. Ding, D. Li, Y. Tang. A low cost cutter-based paper lamination rapid prototyping system. *Int. J. Mach. Tools Manuf.*, 2003, 43(11): 1079–1086
35. D. Ahn, J. H. Kweon, J. Choi, S. Lee. Quantification of surface roughness of parts processed by laminated object manufacturing. *J. Mater. Process. Technol.*, 2012, 212(2): 339–346
36. G. S. Kelly, M. S. Jr Just, S. G. Advani, J. W. Gillespie. Energy and bond strength development during ultrasonic consolidation. *J. Mater. Process. Technol.*, 2014, 214(8): 1665–1672
37. Z. H. Liu, D. Q. Zhang, S. L. Sing, C. K. Chua, L. E. Loh. Interfacial characterization of SLM parts in multi-material processing: Metallurgical diffusion between 316L stainless steel and C18400 copper alloy. *Mater. Charact.*, 2014, 94: 116–125
38. W. Y. Yeong, et al. Porous polycaprolactone scaffold for cardiac tissue engineering fabricated by selective laser sintering. *Acta Biomater.*, 2010, 6(6): 2028–2034
39. C. Guo, W. Ge, F. Lin. Effects of scanning parameters on material deposition during Electron Beam Selective Melting of Ti-6Al-4V powder. *J. Mater. Process. Technol.*, 2015, 217: 148–157
40. T. Durejko, M. Ziętala, W. Polkowski, T. Czujko. Thin wall tubes with Fe_3Al/SS316L graded structure obtained by using laser engineered net shaping technology. *Mater. Des.*, 2014, 63: 766–774
41. M. Gharbi, et al. Influence of various process conditions on surface finishes induced by the direct metal deposition laser technique on a Ti-6Al-4V alloy. *J. Mater. Process. Technol.*, 2013, 213(5): 791–800
42. M. Castilho, et al. Direct 3D powder printing of biphasic calcium phosphate scaffolds for substitution of complex bone defects. *Biofabrication*, 2014, 6(1): 015006
43. A. Butscher, et al. Printability of calcium phosphate powders for three-dimensional printing of tissue engineering scaffolds. *Acta Biomater.*, 2012, 8(1): 373–385
44. A. Butscher, M. Bohner, N. Doebelin, S. Hofmann, R. Müller. New depowdering-friendly designs for three-dimensional printing of calcium phosphate bone substitutes. *Acta Biomater.*, 2013, 9(11): 9149–9158
45. K. C. Ang, K. F. Leong, C. K. Chua, M. Chandrasekaran. Compressive properties and degradability of poly(ε-caprolatone)/hydroxyapatite composites under accelerated hydrolytic degradation. *J. Biomed. Mater. Res. A*, 2007, 80A(3): 655–660
46. C. M. Cheah, K. F. Leong, C. K. Chua, K. H. Low, H. S. Quek. Characterization of microfeatures in selective laser sintered drug delivery devices. *Proc. Inst. Mech. Eng. H*, 2002, 216(6): 369–383
47. K. F. Leong, C. K. Chua, W. S. Gui, Verani. Building porous biopolymeric microstructures for controlled drug delivery devices using selective laser sintering. *Int. J. Adv. Manuf. Technol.*, 2006, 31(5–6): 483–489
48. K. F. Leong, F. E. Wiria, C. K. Chua, S. H. Li. Characterization of a poly-ε-caprolactone polymeric drug delivery device built by selective laser sintering. *Biomed Mater Eng.*, 2007, 17(3): 147–157
49. K. H. Tan, et al. Selective laser sintering of biocompatible polymers for applications in tissue engineering. *Biomed Mater Eng.*, 2005, 15(1–2): 113–124
50. R. L. Simpson, et al. Development of a 95/5 poly(*L*-lactide-*co*-glycolide)/hydroxylapatite and ε-tricalcium phosphate scaffold as bone replacement material via selective laser sintering. *J. Biomed. Mater. Res. B Appl. Biomater.*, 2008, 84B(1): 17–25
51. K. H. Tan, et al. Scaffold development using selective laser sintering of polyetheretherketone-hydroxyapatite biocomposite blends. *Biomaterials*, 2003, 24(18): 3115–3123
52. K. H. Tan, C. K. Chua, K. F. Leong, M. W. Naing, C. M. Cheah. Fabrication and characterization of three-dimensional poly(ether-ether-ketone)/-hydroxyapatite biocomposite scaffolds using laser sintering. *Proc. Inst. Mech. Eng. H*, 2005, 219(3): 183–194
53. C. K. Chua, K. F. Leong, K. H. Tan, F. E. Wiria, C. M. Cheah. Development of tissue scaffolds using selective laser sintering of polyvinyl alcohol/hydroxyapatite biocomposite for craniofacial and joint defects. *J. Mater. Sci. Mater. Med.*, 2004, 15(10): 1113–1121
54. F. E. Wiria, C. K. Chua, K. F. Leong, Z. Y. Quah, M. Chandrasekaran, M. W. Lee. Improved biocomposite development of poly(vinyl alcohol) and hydroxyapatite for tissue engineering scaffold fabrication using selective laser sintering. *J. Mater. Sci. Mater. Med.*, 2008, 19(3): 989–996
55. F. E. Wiria, K. F. Leong, C. K. Chua, Y. Liu. Poly-ε-caprolactone/hydroxyapatite for tissue engineering scaffold fabrication via selective laser sintering. *Acta Biomater.*, 2007, 3(1): 1–12
56. F. E. Wiria, N. Sudarmadji, K. F. Leong, C. K. Chua, E. W. Chng, C. C. Chan. Selective laser sintering adaptation tools for cost effective fabrication of biomedical prototypes. *Rapid Prototyping J.*, 2010, 16(2): 90–99
57. G. Kim, J. Son, S. Park, W. Kim. Hybrid process for fabricating 3D hierarchical scaffolds combining rapid prototyping and electrospinning. *Macromol. Rapid Commun.*, 2008, 29(19): 1577–1581
58. S. H. Park, U. H. Koh, M. Kim, D. Y. Yang, K. Y. Suh, J. H. Shin. Hierarchical multilayer assembly of an ordered nanofibrous scaffold via thermal fusion bonding. *Biofabrication*, 2014, 6(2): 024107
59. C. H. Chen, V. B. H. Shyu, J. P. Chen, M. Y. Lee. Selective laser sintered poly-ε-caprolactone scaffold hybridized with collagen hydrogel for cartilage tissue engineering. *Biofabrication*, 2014, 6(1): 015004

60. C. K. Chua, M. W. Naing, K. F. Leong, C. M. Cheah. Novel method for producing polyhedra scaffolds in tissue engineering. In: *Virtual Modeling and Rapid Manufacturing—Advanced Research in Virtual and Rapid Prototyping*, 2003: 633–640
61. H. S. Ramanath, C. K. Chua, K. F. Leong, K. D. Shah. Melt flow behaviour of poly-ε-caprolactone in fused deposition modelling. *J. Mater. Sci. Mater. Med.*, 2008, 19(7): 2541–2550
62. F. E. Wiria, K. F. Leong, C. K. Chua. Modeling of powder particle heat transfer process in selective laser sintering for fabricating tissue engineering scaffolds. *Rapid Prototyping J.*, 2010, 16(6): 400–410
63. K. C. Ang, K. F. Leong, C. K. Chua, M. Chandrasekaran. Investigation of the mechanical properties and porosity relationships in fused deposition modeling-fabricated porous structures. *Rapid Prototyping J.*, 2006, 12(2): 100–105
64. H. S. Ramanath, M. Chandrasekaran, C. K. Chua, K. F. Leong, K. D. Shah. Modeling of extrusion behavior of biopolymer and composites in fused deposition modeling. In: *Key Engineering Materials*, 2007, 334–335: 1241–1244
65. N. Sudarmadji, J. Y. Tan, K. F. Leong, C. K. Chua, Y. T. Loh. Investigation of the mechanical properties and porosity relationships in selective laser-sintered polyhedral for functionally graded scaffolds. *Acta Biomater.*, 2011, 7(2): 530–537
66. C. E. Misch, Z. Qu, M. W. Bidez. Mechanical properties of trabecular bone in the human mandible: Implications for dental implant treatment planning and surgical placement. *J. Oral Maxillofac. Surg.*, 1999, 57(6): 700–706, discussion 706–708
67. C. K. Chua, M. J. J. Liu, S. M. Chou. Additive manufacturing-assisted scaffold-based tissue engineering. In: *Innovative Developments in Virtual and Physical Prototyping—Proceedings of the 5th International Conference on Advanced Research and Rapid Prototyping*, 2012: 13–21
68. W. Y. Yeong, C. K. Chua, K. F. Leong, M. Chandrasekaran, M. W. Lee. Indirect fabrication of collagen scaffold based on inkjet printing technique. *Rapid Prototyping J.*, 2006, 12(4): 229–237
69. W. Y. Yeong, C. K. Chua, K. F. Leong, M. Chandrasekaran, M. W. Lee. Comparison of drying methods in the fabrication of collagen scaffold via indirect rapid prototyping. *J. Biomed. Mater. Res. B Appl. Biomater.*, 2007, 82B(1): 260–266
70. J. Y. Tan, C. K. Chua, K. F. Leong. Indirect fabrication of tissue engineering scaffolds using rapid prototyping and a foaming process. In: *Innovative Developments in Design and Manufacturing—Advanced Research in Virtual and Rapid Prototyping*, 2010: 51–57
71. J. Y. Tan, C. K. Chua, K. F. Leong. Fabrication of channeled scaffolds with ordered array of micro-pores through microsphere leaching and indirect Rapid Prototyping technique. *Biomed. Microdevices*, 2013, 15(1): 83–96
72. C. H. Chen, J. M. J. Liu, C. K. Chua, S. M. Chou, V. B. H. Shyu, J. P. Chen. Cartilage tissue engineering with silk fibroin scaffolds fabricated by indirect additive manufacturing technology. *Materials (Basel)*, 2014, 7(3): 2104–2119
73. V. Mironov, V. Kasyanov, R. R. Markwald. Organ printing: From bioprinter to organ biofabrication line. *Curr. Opin. Biotechnol.*, 2011, 22(5): 667–673
74. M. Bartnikowski, T. J. Klein, F. P. W. Melchels, M. A. Woodruff. Effects of scaffold architecture on mechanical characteristics and osteoblast response to static and perfusion bioreactor cultures. *Biotechnol. Bioeng.*, 2014, 111(7): 1440–1451
75. M. Ghaedi, J. J. Mendez, P. F. Bove, A. Sivarapatna, M. S. B. Raredon, L. E. Niklason. Alveolar epithelial differentiation of human induced pluripotent stem cells in a rotating bioreactor. *Biomaterials*, 2014, 35(2): 699–710
76. T. W. G. M. Spitters, et al. A dual flow bioreactor with controlled mechanical stimulation for cartilage tissue engineering. *Tissue Eng. Part C Methods*, 2013, 19(10): 774–783
77. L. Dan, C. K. Chua, K. F. Leong. Fibroblast response to interstitial flow: A state-of-the-art review. *Biotechnol. Bioeng.*, 2010, 107(1): 1–10
78. D. Liu, C. K. Chua, K. F. Leong. A mathematical model for fluid shear-sensitive 3D tissue construct development. *Biomech. Model. Mechanobiol.*, 2013, 12(1): 19–31
79. B. C. M. Tay, C. Y. Fu, B. K. Ng, J. M. J. Liu, S. M. Chou, C. K. Chua. Monitoring cell proliferation in silk fibroin scaffolds using spectroscopic optical coherence tomography. *Microw. Opt. Technol. Lett.*, 2013, 55(11): 2587–2594
80. C. K. Chua, W. Y. Yeong. *Bioprinting: Principles and Applications*. Singapore: World Scientific Publishing Company Pte Limited, 2014
81. V. Mironov, T. Boland, T. Trusk, G. Forgacs, R. R. Markwald. Organ printing: Computer-aided jet-based 3D tissue engineering. *Trends Biotechnol.*, 2003, 21(4): 157–161
82. V. Mironov, V. Kasyanov, C. Drake, R. R. Markwald. Organ printing: Promises and challenges. *Regen. Med.*, 2008, 3(1): 93–103
83. V. Mironov, R. P. Visconti, V. Kasyanov, G. Forgacs, C. J. Drake, R. R. Markwald. Organ printing: Tissue spheroids as building blocks. *Biomaterials*, 2009, 30(12): 2164–2174
84. J. An, C. K. Chua, T. Yu, H. Li, L. P. Tan. Advanced nanobiomaterial strategies for the development of organized tissue engineering constructs. *Nanomedicine (Lond)*, 2013, 8(4): 591–602
85. Alec. Russian scientists to unveil 3D bioprinted transplantable organ in March 2015. 2014-11-10. http://www.3ders.org/articles/20141110-russian-scientists-to-unveil-3d-bioprinted-transplantable-organ-in-march-2015.html
86. S. V. Murphy, A. Atala. 3D bioprinting of tissues and organs. *Nat. Biotechnol.*, 2014, 32(8): 773–785
87. D. B. Kolesky, R. L. Truby, A. S. Gladman, T. A. Busbee, K. A. Homan, J. A. Lewis. 3D bioprinting of vascularized, heterogeneous cell-laden tissue constructs. *Adv. Mater.*, 2014, 26(19): 3124–3130
88. N. E. Fedorovich, et al. Biofabrication of osteochondral tissue equivalents by printing topologically defined, cell-laden hydrogel scaffolds. *Tissue Eng. Part C Methods*, 2012, 18(1): 33–44
89. J. M. Lee, W. Y. Yeong. A preliminary model of time-pressure dispensing system for bioprinting based on printing and material parameters. In: *Virtual and Physical Prototyping*, 2014: 1–6
90. C. Cvetkovic, et al. Three-dimensionally printed biological machines powered by skeletal muscle. *Proc. Natl. Acad. Sci. U.S.A.*, 2014, 111(28): 10125–10130
91. S. Tibbits. 4D printing: Multi-material shape change. *Architectural Design*, 2014, 84(1): 116–121
92. Q. Ge, C. K. Dunn, H. J. Qi, M. L. Dunn. Active origami by 4D printing. In: *Smart Materials and Structures*, 2014, 23: 094007–094022
93. E. Pei. 4D printing—Revolution or fad? *Assembly Automation*, 2014, 34(2): 123–127
94. E. M. Teoh, C. K. Chua, Y. Liu, D. Q. Zhang. Four dimensional (4D) printing using polyjet technology. In: *The 4th International Conference on Additive Manufacturing and Bio-manufacturing (ICAM-BM 2014)*. Beijing, China, 2014: 35–36
95. R. W. Esmond, G. C. Phero. The additive manufacturing revolution and the corresponding legal landscape. In: *Virtual and Physical Prototyping*, 2014: 1–4